Frontiers of Information Technology & Electronic Engineering
www.jzus.zju.edu.cn; engineering.cae.cn; www.springerlink.com
ISSN 2095-9184 (print); ISSN 2095-9230 (online)
E-mail: jzus@zju.edu.cn

*Review:*

# Graphene-based silicon modulators*

Hao-wen SHU[1,2], Ming JIN[1,2], Yuan-sheng TAO[1,2], Xing-jun WANG‡[1,2]

[1]*State Key Laboratory on Advanced Optical Communication Systems and Networks, Department of Electronics, School of Electronics Engineering and Computer Science, Peking University, Beijing 100871, China*

[2]*Nano-optoelectronics Frontier Center of Ministry of Education at Peking University, Beijing 100871, China*

E-mail: haowenshu@pku.edu.cn; mjin@pku.edu.cn; ystao@pku.edu.cn; xjwang@pku.edu.cn

Received June 28, 2018; Revision accepted Nov. 16, 2018; Crosschecked Apr. 11, 2019

**Abstract:** Silicon photonics is a promising technology to address the demand for dense and integrated next-generation optical interconnections due to its complementary-metal-oxide-semiconductor (CMOS) compatibility. However, one of the key building blocks, the silicon modulator, suffers from several drawbacks, including a limited bandwidth, a relatively large footprint, and high power consumption. The graphene-based silicon modulator, which benefits from the excellent optical properties of the two-dimensional graphene material with its unique band structure, has significantly advanced the above critical figures of merit. In this work, we review the state-of-the-art graphene-based silicon modulators operating in various mechanisms, i.e., thermal-optical, electro-optical, and plasmonic. It is shown that graphene-based silicon modulators possess the potential to have satisfactory characteristics in intra- and inter-chip connections.

**Key words:** Silicon photonics; Graphene; Optical modulator
https://doi.org/10.1631/FITEE.1800407 **CLC number:** O436.4

## 1 Introduction

The rapidly growing volume of data in intra- and inter-chip connections, especially in data centers, requires transceivers with higher operational speeds (>25 Gbaud) and lower power consumption (<1 pJ/bit) (Thomson et al., 2016). Silicon photonics, compared with conventional electrical interconnection approaches, presents strengths in both bandwidth and loss, which are always performance bottlenecks with copper cables in the gigahertz data frequency (Reed et al., 2010). To address the growing demands for data transmission, high-speed silicon modulators have been extensively studied for short-range interconnections and long-haul communications (Jones et al., 2004; Liu et al., 2004; Chen et al., 2011; Li et al., 2013). While the silicon is transparent for transmission within the C band, limitations still exist in each modulation structure of silicon modulators. For Mach-Zehnder interferometer (MZI) based silicon modulators, the relatively weak plasma dispersion effect in silicon modulators leads to a millimeter-scale device length. Such a long modulator demands a traveling wave electrode, whose bandwidth is always suppressed by the impedance mismatch and group-velocity mismatch (GVM) between light waves and microelectronic waves (Chen et al., 2012). As for microring-based silicon modulators, the remarkable thermal center wavelength shifts always necessitate an external temperature control scheme, which increases the complexity of system design.

To increase the operation speed and simplify the size of a conventional silicon modulator, some promising approaches have been reported by

‡ Corresponding author

* Project supported by the National Natural Science Foundation of China (Nos. 61535002 and 61635001)

ORCID: Xing-jun WANG, http://orcid.org/0000-0001-8206-2544

assembling the silicon waveguide with other materials, such as polymer, metal, and two-dimensional (2D) materials (Liu et al., 2011; Haffner et al., 2015; Koeber et al., 2015; Shu et al., 2018a). The polymer-based silicon waveguide, generally with a high electro-optical effect index, can reach modulation efficiencies up to 0.5 V·mm. The silicon-oxide-metal hybrid structures dramatically scale down the footprint and power consumption of a device with their strong confinement of light. Even so, such silicon organic hybrid (SOH) and surface plasmonic polariton (SPP) modulators encounter many problems in manufacturing (such as the stability of polymer and the high requirement of precision in metal growth). Among the aforementioned 2D materials, graphene, a monolayer material of only 0.34-nm thickness, exhibits remarkable characteristics in both amplitude and phase control of light in several modulation mechanisms. The transport characteristics and conductivity of graphene can be tuned conveniently by electrical injection (Novoselov et al., 2004; Hanson, 2008; Li et al., 2008; Wang et al., 2008; Xu et al., 2015). Thus, a graphene-based structure is suitable for electro-optical (E-O) modulation. For thermal-optical (T-O) effect, the thermal conductivity of graphene, as high as 5300 W/(m·K) (Balandin et al., 2008; Pop et al., 2012; Yin et al., 2018), is larger than that of any other known material in nature. Hence, graphene can act as an efficient micro-heater or heat-conducting medium in a T-O modulator. Moreover, the graphene plasmonic effect would be stimulated in some conditions, which improves the modulation efficiency prodigiously (Dionne et al., 2009). Furthermore, the transfer technology of monolayer graphene onto the silicon waveguide surface is within several steps and is compatible with the complementary-metal-oxide-semiconductor (CMOS) technology. As for the graphene modulators fabricated under the integrated silicon photonics technology, the devices have superiority of their compact size (about 100 μm$^2$), high speed in multi-gigahertz, and great manufacturing potential because of their CMOS compatibility.

In this work, we present a comprehensive survey of recent progress in graphene-based silicon modulators with different operational mechanisms, such as E-O, T-O, and all-optical, as well as graphene plasmonic (GP) effects. Each figure of merit (FOM) for modulators, such as the footprint, modulation efficiency, bandwidth, and power consumption, is well summarized and analyzed. The performance of these graphene-based devices shows their potential for the future of optical integrated circuits for long-haul communications and data center interconnections.

## 2 Electro-optical (E-O) graphene silicon modulators

### 2.1 Modulation theory

The excellent electrical properties of graphene, such as high carrier mobility and tunable electrical conductivity, have been extensively studied because graphene allows a high speed and broadband light modulation (Novoselov et al., 2004; Hanson, 2008; Li et al., 2008; Wang et al., 2008; Xu et al., 2015; Sorianello et al., 2016). Graphene's band structure, together with its extreme thinness, leads to a pronounced electric field effect to electrically control the light properties (Novoselov et al., 2004). The Kubo formula (Hanson, 2008) reveals that the real- and imaginary-part changes of the complex conductivity in graphene thin film will result in the absorption and phase shift of an optical signal pulse, respectively (Li et al., 2008; Wang et al., 2008), as shown in the following equation:

$$\sigma(\omega,\mu_{\mathrm{c}},\Gamma,T)=\frac{\mathrm{j}e^2(\omega-\mathrm{j}2\Gamma)}{\pi\hbar^2}\cdot\left[\frac{1}{(\omega-\mathrm{j}2\Gamma)^2}\int_0^{+\infty}\xi\left(\frac{\partial f_d(\xi)}{\partial\xi}-\frac{\partial f_d(-\xi)}{\partial\xi}\right)\mathrm{d}\xi-\int_0^{+\infty}\frac{f_d(-\xi)-f_d(\xi)}{(\omega-\mathrm{j}2\Gamma)^2-4(\xi/\hbar)^2}\mathrm{d}\xi\right],\tag{1}$$

where $\omega$, $\mu_{\mathrm{c}}$, $\Gamma$, and $T$ represent the radian frequency, chemical potential, carrier relaxation time, and temperature, respectively. $f_d(\xi)=(\mathrm{e}^{(\xi-\mu_{\mathrm{c}})/(k_{\mathrm{B}}T)}+1)^{-1}$ is the Fermi-Dirac distribution, where $\xi$ is the energy and $k_{\mathrm{B}}$ the Boltzmann constant. Through calculation, the formula indicates that graphene modulators can be switched between the electro-absorptive mode and electro-refractive mode (Fig. 1). Within the chemical potential range from 0 to 1 eV, the absorption and effective indexes of a silicon-graphene hybrid structure operating in 1550 nm exhibit three different sets of characteristics. The yellow area is the absorption region, wherein the absorption remains high and both the effective and

absorption indexes change very little. For the step change region, there is a significant "stepping up" for the absorption index. Consequently, intensive modulation is suitable within the range. Phase modulation fits well in the linear region since the absorption is low and the effective index exhibits a linear change. Such a theoretical mechanism has been experimentally verified on the silicon platform by several works recently (Xu et al., 2015; Sorianello et al., 2016). So far, the graphene-silicon electro-optical modulators have focused mainly on intensity modulation based on the electro-absorption effect. More recently, some experimental work on the electro-refractive effect has been reported, indicating the possibility of phase modulation by electrical injection.

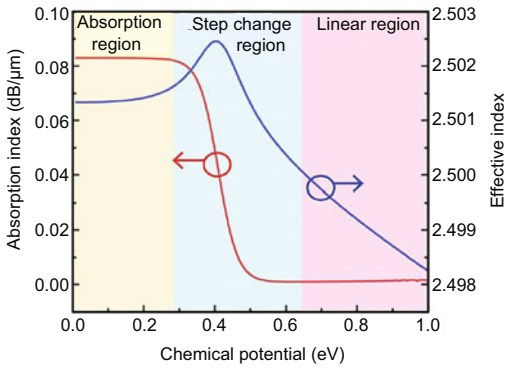


**Fig. 1 Complex effective index of the graphene-oxide-silicon waveguide in 1550 nm resulting from the Kubo formula (Shu et al. (2018b), licensed under CC BY 4.0). References to color refer to the online version of this figure**

## 2.2 Typical structure

For a typical E-O graphene-silicon modulator, the graphene is transferred mainly to the top of an integrated passive photonics structure, such as a single silicon waveguide, Mach-Zehnder interferometer, or the microring resonator, to manipulate the evanescent light wave coupled from the waveguide. The first prototype of E-O graphene was reported in Liu et al. (2011), in which modulation was achieved by actively tuning the Fermi level of a monolayer graphene sheet (Fig. 2a). The graphene layer, alumina oxide layer, and silicon waveguide were proposed in the paper, forming the graphene-oxide-silicon (GOS) capacitance structure. Subsequently, to eliminate the optical loss widely existing in silicon photonics, the demonstration of the GOG (graphene-oxide-graphene) structure (Fig. 2b) was reported in Liu et al. (2012), for lower energy consumption and insertion loss. These two types of the electro-optic interaction region are the mainstream design in later research works.

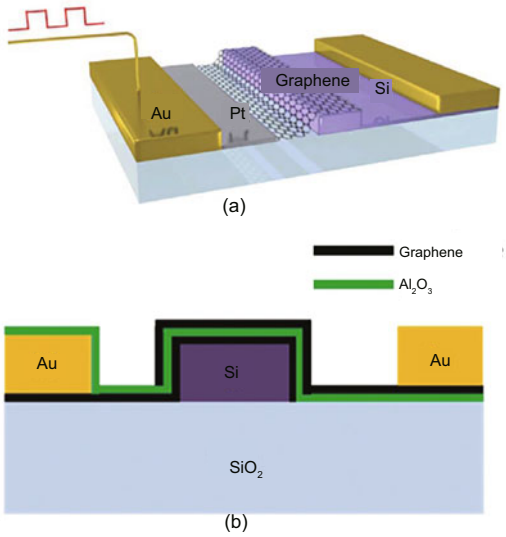


**Fig. 2 Two typical structures of graphene based silicon strip waveguide modulators: (a) graphene-oxide-silicon (GOS) waveguide modulator (reprinted from Liu et al. (2011), Copyright 2011, with permission from Springer); (b) graphene-oxide-graphene (GOG) waveguide modulator (reprinted from Liu et al. (2012), Copyright 2012, with permission from American Chemical Society)**

To enhance the interaction between the propagating light and the graphene, the GOS modulator based on a slot waveguide was proposed with the slot orientation as either horizontal (Fig. 3a) (Phatak et al., 2016) or vertical (Ye et al., 2017), because most of the light energy is confined in the silicon waveguide with a weak evanescent wave leaking from it. Another way for interaction enhancement is to introduce a microring taking the place of the single waveguide as the passive optical substrate (Qiu et al., 2014; Ding et al., 2015; Phare et al., 2015). A higher integration level, extinction ratio, and operational speed can be achieved due to resonator loss modulation at the critical coupling of the microring. A 30-GHz GOG modulator (Fig. 3b) (Phare et al., 2015) and high modulation depth GOS modulators (Qiu et al., 2014; Ding et al., 2015) based on a microring resonator were demonstrated, showing that the speed and efficiency can be drastically increased.

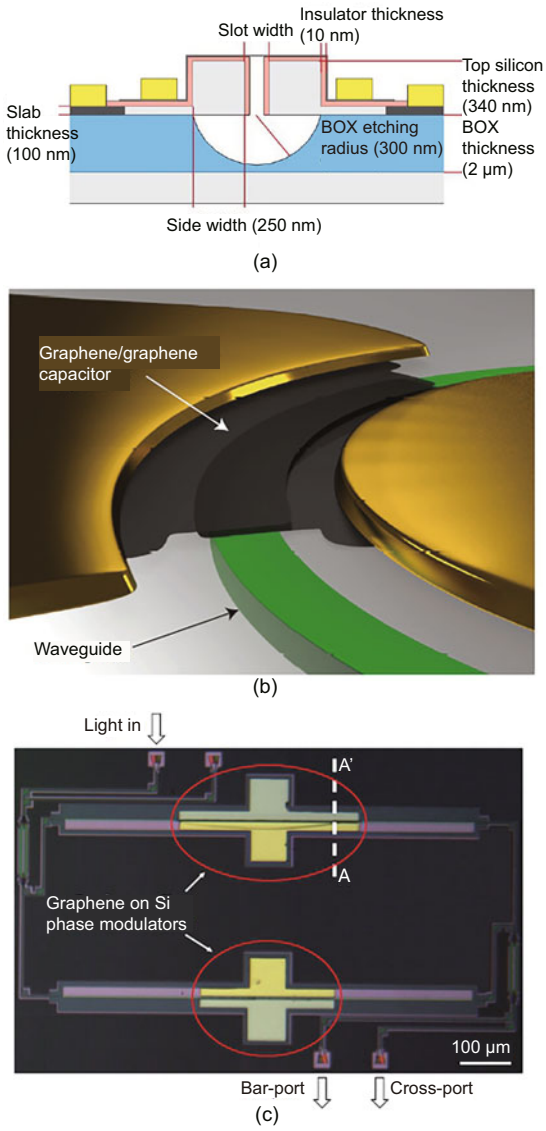


**Fig. 3 Several optical constructions for higher performance in the graphene-based silicon modulator: (a) slot waveguide (reprinted from Phatak et al. (2016), Copyright 2016, with permission from The Optical Society); (b) microring (reprinted from Phare et al. (2015), Copyright 2015, with permission from Springer); (c) Mach-Zehnder interferometer (reprinted from Sorianello et al. (2018), Copyright 2017, with permission from Springer)**

All the modulators listed above, which focus mainly on intensity modulation, are suitable for short-range interconnections in data centers. For long-haul coherent communications, phase modulation is essential. The graphene-phase modulators based on MZI were successively proposed (Mohsin et al., 2015; Shu et al., 2018b; Sorianello et al., 2018). The Kubo formula and the Maxwell equations indicate that the optical conductivity of graphene can be controlled through the applied voltage (Xu et al., 2012). The GOG graphene-phase modulator was first experimentally demonstrated in Mohsin et al. (2015), with a 300-V·mm modulation efficiency and a multi-megahertz operation speed. A more efficient modulator (1.29 V·mm) (Shu et al., 2018b) and a higher speed (5 GHz, as shown in Fig. 3c) (Sorianello et al., 2018) phase modulator with the ability to change modes, were demonstrated subsequently based on a GOS structure, heralding the potential application of graphene modulators in both optical communications and interconnection systems.

### 2.3 Device performance

The footprint, modulation efficiency, bandwidth, and power consumption are the most crucial FOMs for modulators. In integrated silicon photonic systems, the race for the perfect modulator is still open, as none of the actual devices including MZI-based modulators or silicon ring modulators show sufficient values for all of the parameters mentioned (Mohsin et al., 2015). For silicon-based MZI modulators, the device footprint is on the order of millimeters, owing to its weak plasma dispersion effect (Liu et al., 2004). The electro-refractive effect of the graphene layer can be used to change the refractive index $\Delta n$ of Si larger than $10^{-3}$, almost 30 times larger than that of a carrier depletion mode modulator (Soref and Larenzo, 1986; Sorianello et al., 2016). The length of the interaction region in a graphene MZI modulator arm is within 10–300 μm (Wang et al., 2008; Pop et al., 2012; Xu et al., 2015), about $\frac{1}{100}$–$\frac{1}{10}$ that of the silicon MZI modulator. The size of a microring-based graphene modulator is generally determined by the resonator structure. A larger radius of the ring resonator may help reduce the transfer precision. Thus, a 40-μm ring resonator (Novoselov et al., 2004) and a 50-μm one (Hanson, 2008) were fabricated with an experimental result showing higher speed and efficiency. Modulation efficiency is defined as the modulation depth (or extinction ratio) and $V_\pi L_\pi$ for the type of modulator to be electro-absorptive and electro-refractive, respectively. The common modulation depth of a GOS structure is about 0.1 dB/μm (Liu et al., 2011). For GOG, the value is about 0.16 dB/μm (Liu et al., 2012), which has a positive correlation with the

number of graphene layers. The first microring graphene modulator had an extinction ratio of about 40% (Qiu et al., 2014), in which the graphene film covered the whole resonator structure. Higher modulation depths, 15 dB per 10 V (Novoselov et al., 2004) and 12.5 dB per 8.8 V (Hanson, 2008), were demonstrated by tuning the loss of the graphene-silicon interaction region only on part of the ring designed in the critical coupling scheme. $V_\pi L_\pi$ is considered in the modulators using the electro-refractive effect. The first experimental phase modulator maintained $V_\pi L_\pi$ of 30 V·cm, which is comparable to that of Si-based phase modulators, where typical values in the range of 0.5–15 V·cm were achieved (Mohsin et al., 2015). By reducing the thickness of the oxide layer which is sandwiched between the graphene layer and the silicon waveguide, a higher $V_\pi L_\pi$ could be achieved to 0.28 V·cm (Sorianello et al., 2018) and 0.13 V·cm (Xu et al., 2015).

The modulation bandwidth is one of the most important FOMs for an optical modulator. The modulation bandwidth is usually defined by the frequency at which the optic field is reduced to 50% of its maximum value (Reed et al., 2010). The bandwidth of a graphene-silicon electro-optical modulator is limited mainly by the resistor-capacitor (RC) constant of the interaction region, in which the graphene-electrode contact resistance and dielectric capacitance are the major factors determining the RC constant (Sorianello et al., 2015). The contact resistance depends directly on the growth technology of the electrode, while the dielectric capacitance is determined mainly by the thickness of the dielectric oxide of the capacitance structure in the interaction region (Phare et al., 2015). Before 2016, the bandwidth of the absorption mode graphene modulator based on the waveguide or MZI was lower than 1 GHz (Chen et al., 2012; Mohsin et al., 2014; Koeber et al., 2015), the performance of the ring modulator was relatively good, and a 30-GHz bandwidth could be realized in the silicon-nitride platform (Phare et al., 2015). More recently, an athermal GOG MZI absorption modulator was demonstrated with a bandwidth as high as 35 GHz (Dalir et al., 2016), as shown in Figs. 4a and 4b. For phase modulators, Figs. 4c and 4d illustrate the schematic and the eye diagram of a graphene-based MZI modulator with the fastest operation speed (about 10 Gb/s) so far. To optimize the RC constant, the double-layer graphene is located beneath the amorphous silicon, which helps achieve a 10 times thicker spacer layer between graphene layers. Nevertheless, the theoretically calculated bandwidth of the graphene E-O modulator could be as high as 100 GHz (Gosciniak and Tan, 2013b; Ye et al., 2017), which shows a great potential for promotion.

For the assessment of any interconnection solution, power consumption is a vital factor. The average power consumption of a modulator is given by $(CV)^2/4$ (Miller, 2012), where $C$ is the modulator capacitance and $V$ the dynamic voltage variation. The power consumption of the GOS structure in Sorianello et al. (2018) is about 1 pJ/bit, while the GOG structure in Phare et al. (2015) holds a relatively low energy consumption of 800 fJ/bit because of the halved driven voltage of the GOG scheme (Sorianello et al., 2015). Both schemes keep the power consumption lower than 1 pJ/bit, which fulfills the need of future interconnection systems (Miller, 2009).

## 3 Thermo-optical (T-O) graphene silicon modulators

In addition to the E-O effect, thermo-optical (T-O) modulation is an alternative approach for low-frequency applications since silicon exhibits a large T-O coefficient ($\mathrm{d}n/\mathrm{d}T$) as high as $(1.86 \pm 0.08) \times 10^{-4}\ \mathrm{K}^{-1}$ (Cocorullo and Rendina, 1992; Reed et al., 2010). The change in the refractive index of silicon caused by the T-O effect can be distinctly expressed as $\Delta n = (\mathrm{d}n/\mathrm{d}T) \cdot \Delta T$, in which $\Delta T$ is the variation of the temperature. Thermal tuning for an all-silicon modulator is often applied using a metallic micro-heater on a silicon waveguide. However, a thick silicon dioxide layer is generally sandwiched between the silicon and the heater to avoid light-absorption loss induced by the metal in the design of an all-silicon modulator. Such a thick $SiO_2$ layer keeps the heat source far away from the modulation region and its thermal conductivity (1.44 W/(m·K)) (Yamane et al., 2002) is about 1/100 that of silicon (about 149 W/(m·K)) (Liu and Asheghi, 2005); thus, the T-O response speed and the heating efficiency decrease.

Among all known materials, the graphene has the highest in-plane thermal conductivity at room temperature, which can be up to 5300 W/(m·K) (Balandin et al., 2008; Pop et al., 2012). The direct

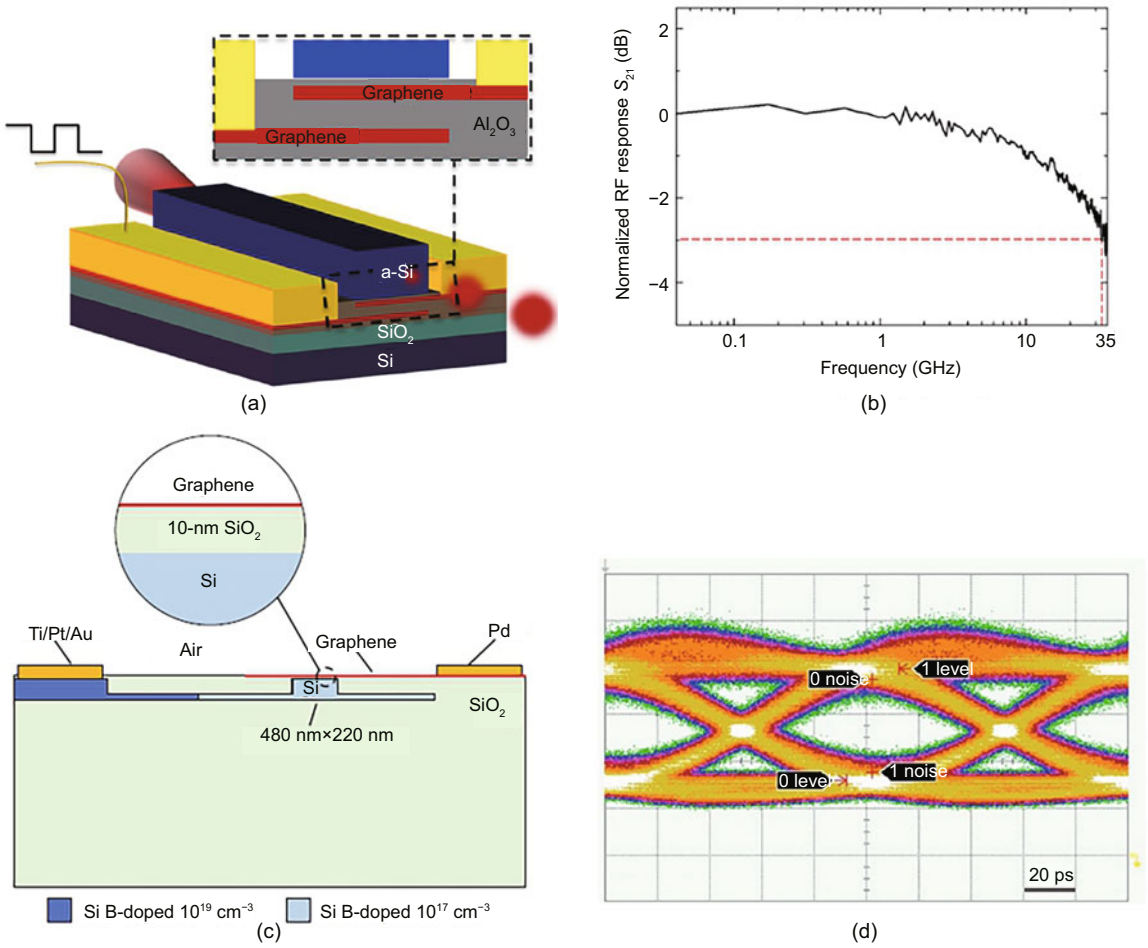


**Fig. 4 Structure schematic of the graphene-silicon intensity modulator (a) (reprinted from Dalir et al. (2016), Copyright 2016, with permission from American Chemical Society), bandwidth of the absorption modulator (b) (reprinted from Dalir et al. (2016), Copyright 2016, with permission from American Chemical Society), cross-section illustration of the graphene-silicon phase modulator (c) (reprinted from Sorianello et al. (2018), Copyright 2017, with permission from Springer), and 10-Gb/s eye diagram of the phase modulator (d) (reprinted from Sorianello et al. (2018), Copyright 2017, with permission from Springer)**

contact of the graphene heater with the silicon waveguide eliminates the drawbacks of poor thermal conductivity introduced by the thick $SiO_2$ layer, thus enhancing the heating efficiency. Such T-O graphene-silicon modulators were first demonstrated in Kim et al. (2013), based on a graphene plasmonic waveguide (Fig. 5a). The graphene plasmonic waveguide and graphene heater were configured together for the purposes of compact device design and fabrication. A 30-dB attenuation at a telecom wavelength with 12-mW electrical power injection has been demonstrated.

This kind of graphene-silicon integrated modulator has a typical structure (Fig. 5b), i.e., a thermal tuning MZI structure by using graphene as the transparent flexible heat conductor on one of modulation arms (Yu et al., 2014). The graphene heat conductor is used to deliver heat from metal heaters to the silicon waveguide arm. A 7-nm red shift of the spectra was achieved under the injection electrical power of 110 mW at a 1-kHz modulation rate. The 90% rising and decaying time (defined as the time it takes for the change in temperature to reach 90% (from zero) or 10% (from peak) of the maximum value) is 20 μs.

To increase the response time and heating efficiency, several novel structures have been proposed and demonstrated experimentally, such as photonic

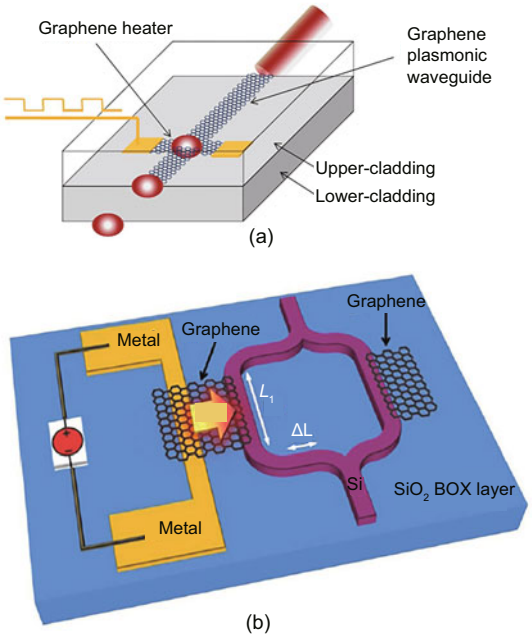


**Fig. 5 Schematic view of the proposed graphene-microribbon-based thermo-optic mode: (a) the long range surface plasmonic polariton (SPP) stripe mode that propagates along the graphene stripe is extinguished (or perturbed) by thermally inducing an inhomogeneous refractive-index distribution (reprinted from Kim et al. (2013), Copyright 2013, with permission from The Optical Society); (b) 3D schematic illustration of a thermally tuning Mach-Zehnder interferometer (MZI) with a non-local traditional metal heater and a graphene-based transparent flexible heat conductor (reprinted from Yu et al. (2014), Copyright 2014, with permission from AIP Publishing)**

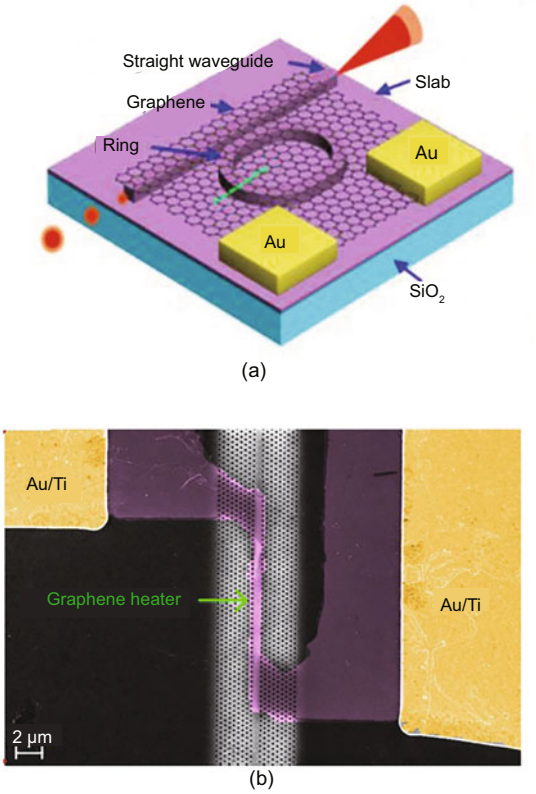


**Fig. 6 Illustration of a thermo-optic microring modulator based on graphene: (a) the monolayer graphene is on top of a ring resonator without any separation layer (reprinted from Gan et al. (2015), Copyright 2015, with permission from Royal Society of Chemistry); (b) false-color scanning electron microscope image of a slow-light-enhanced graphene microheater (Yan et al. (2017), licensed under CC BY 4.0)**

crystal, microring resonator, and microdisk (Gan et al., 2015; Yu et al., 2016; Xu et al., 2017; Yan et al., 2017). A thermal-tuning microring modulator has been demonstrated with a graphene heater covering the whole structure, as shown in Fig. 6a (Gan et al., 2015). The device exhibits a 2.9-nm ring resonator shift under an electrical power of 28 mW, enabling a 7-dB extinction ratio for intensity modulation, and the 90% rising and decaying times are as low as 750 ns (for positive edge) and 800 ns (for negative edge), respectively. Moreover, enhancement of the heating efficiency could be realized by introducing the slow light effect of the silicon photonic crystal waveguide; the scanning electron microscope (SEM) image is shown in Fig. 6b (Yan et al., 2017). A large tuning efficiency of 1.07 nm/mW was reported with 750 ns and 525 ns for the 90% rising and decaying times, respectively, by artfully patterning the shape of the graphene heater, showing the potential for applications in integrated silicon photonics. A silicon photonic crystal nanobeam (PCN) cavity with a graphene micro-heater was demonstrated. Due to the ultra-small optical mode volume ascribed to PCN cavity, the light-matter interaction is improved significantly and heating efficiency is enhanced, reaching 1.5 nm/mW in measurement and 3.75 nm/mW in simulation (Xu et al., 2017).

## 4 All-optical graphene silicon modulators

All-optical modulation controls light through light. The missing part of the conversion between optical signals and electronic signals results in an advantage in power-efficient integrated photonic

systems compared to electronic systems (Qiu et al., 2017). An all-optical graphene-based modulator was primitively realized in graphene-cladded microfiber (Li et al., 2014), which achieved ultrafast optical modulation with a response time at the picosecond scale. This work shows great potential for fiber-optic communication systems in practical applications.

For an all-optical modulator based on a graphene-silicon hybrid integrated platform, a graphene-cladded silicon photonic crystal cavity was demonstrated experimentally, as shown in Fig. 7a (Shi et al., 2015). A 1064-nm continuous-wave laser was used to illuminate the hybrid cavity directly.

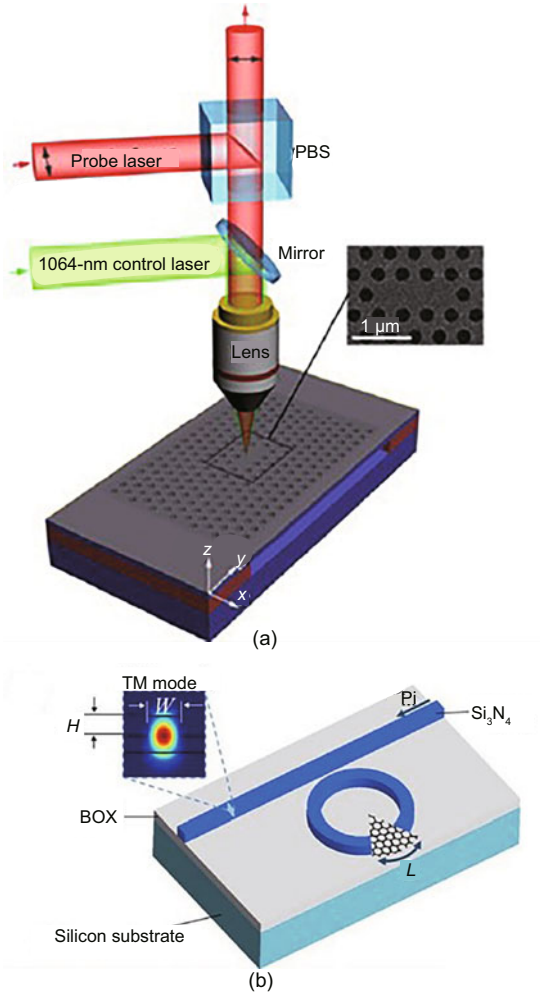


**Fig. 7 Three-dimensional schematic of a graphene-cladded silicon photonic crystal cavity and the measurement setup (a) (reprinted from Shi et al. (2015), Copyright 2015, with permission from American Chemical Society) and that of a graphene-on-$Si_3N_4$ ring resonator device (b) (reprinted from Gao et al. (2017), Copyright 2017, with permission from The Optical Society)**

Due to several mechanisms, such as the optically induced transparency (OIT) effect, free carrier absorption, and free carrier dispersion, a 3.5-nm resonance wavelength shift and a 20% Q-factor change were observed. In addition to a graphene-silicon hybrid platform, a graphene-on-$Si_3N_4$ ring resonator was designed and studied experimentally, as shown in Fig. 7b (Gao et al., 2017).

By engineering the coverage of a graphene layer, a cavity-enhanced T-O bistability was observed. The optical bistability can be used for controlling light with light; therefore, this hybrid resonator has potential for on-chip all-optical modulators. A similar structure was realized on a graphene-on-$Si_3N_4$ platform to investigate an all-optical modulation using the T-O effect, as shown in Fig. 8a (Qiu et al., 2017). The graphene contacts the $Si_3N_4$ waveguide directly; hence, it achieves highly efficient heat transfer from graphene to the waveguide and compensates for the weak T-O effect of the $Si_3N_4$ material. Fig. 8b shows the result of a pump-probe all-optical modulation measurement. The waveform of probe output exhibits a switch between the "off-state" and "on-state" induced by the pump pulse, and the switching time of this device is only 253 ns.

## 5 Plasmonic graphene silicon modulators

SPPs allow the realization of compact optical devices with low energy consumption and a high integration level by confining the light beam in subwavelength-scale dimensions (Dionne et al., 2009; Gosciniak and Tan, 2013a; Li and Yu, 2013). During the last decade, various graphene plasmonic modulators have been demonstrated covering multiple applications, from near-infrared to long-wave infrared (Andersen, 2010; Das et al., 2015), from spatial light to waveguide light modulation (Yan et al., 2012; Gosciniak and Tan, 2013a; Lao et al., 2014), and from graphene self-induced plasmon to metal graphene hybrid excitation plasmon modulators (Andersen, 2010; Yan et al., 2012; Gosciniak and Tan, 2013a; Li and Yu, 2013; Lao et al., 2014; Das et al., 2015). As previously mentioned, in E-O graphene-silicon modulators, graphene interacts primarily with the evanescent wave of a silicon passive optical circuit to achieve electro-absorption and electro-phase modulation. Due to the high refractive

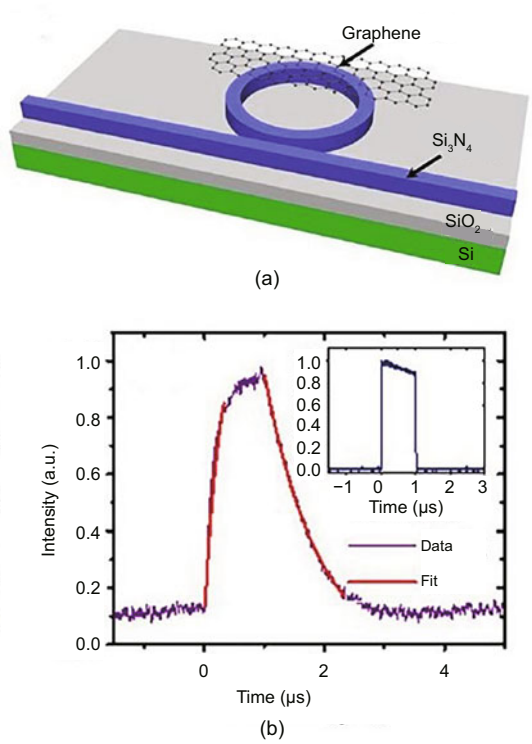


**Fig. 8 Schematic of a graphene-$Si_3N_4$ hybrid all-optical modulator (a) and waveform of the probe output induced by a pump pulse (b) (Qiu et al. (2017), licensed under CC BY 4.0)**

index of silicon, most of the light field is confined in the waveguide, while only a small portion exists in the evanescent field (Liu et al., 2011). However, in a graphene-plasmonic modulator, the SPP mode is generally supported by the metal-dielectric interfaces, which also have a much smaller mode volume owing to the extremely high refractive index difference. This compact configuration exhibits a huge enhancement in the interaction between the optical mode and graphene layer, which will significantly improve the modulation depth. Such E-O modulators based on a hybrid graphene plasmonic waveguide have been explored in the last few years (Ansell et al., 2015; Shin and Kim, 2015; Chen et al., 2016; Ding et al., 2017; Hu and Wang, 2017; Xiao et al., 2017; Ono et al., 2018).

Thus far, modulators with hybrid graphene plasmonic waveguides based on both SPPs excited by noble metals (Ansell et al., 2015; Chen et al., 2016; Ding et al., 2017; Hu and Wang, 2017) and graphene SPs (GSPs) (Dionne et al., 2009; Xiao et al., 2017) have been reported. In Ansell et al. (2015), a wedge SPP mode hybrid graphene plasmonic waveguide modulator was demonstrated (Fig. 9). The optical Pauli blocking effect is used to modulate the propagating SPP modes. By shifting the Fermi energy of graphene produced by gating, the graphene's absorption characteristics were changed (Fig. 9a). Because the SPP mode supports only the transversally magnetic (TM) mode, perpendicular electric fields can excite little current in recumbent graphene. To better enhance the absorption, flat plasmons (FPs), corrugated plasmons (CPs), and wedge plasmons (WPs) graphene based modulators were fabricated. The results indicate that the wedge plasmon mode supported by the edge of the planar section of the waveguide could enhance the in-graphene plane fields near the edge of the strip. A high modulation depth ($>$ 0.03 dB/μm) was achieved within the 10-$\mu m^2$ active device area. Except for these remarkable improvements in size compared with the graphene modulator mentioned before, this typical graphene SPP modulator, however, encounters the dilemma of hard integration with other silicon-based chip scale components.

To achieve the goal of integration with other devices, in Ding et al. (2017), a graphene SPP modulator coupled with a silicon waveguide was demonstrated (Fig. 10), which greatly shortened the path towards the monolithically integrated graphene SPP modulator. The leaky mode describes the energy-loss quasi-confined mode while propagating, which is usually avoided in conventional dielectric photonics. In a slot plasmonic waveguide, more leaky modes result in an optic field farther away from the metal, which will decrease the ohmic loss. By combining such a leaky mode based low-loss plasmonic slot waveguide with two-layer graphene, the interaction between graphene and the optic field will be enhanced. Thus, a high-performance E-O modulator was realized. Such devices can reach a higher modulation depth of 0.13 dB/μm, while maintaining the benefit of a compact footprint (a magnitude of 10 microns). The whole extinction ratio is comparable to those of silicon-based waveguide modulators.

Ono et al. (2018) first demonstrated a novel all-optical modulator with a graphene-loaded deep-subwavelength metal-insulator-metal (MIM) waveguide (the size of the air insulator was 60 nm in height and 40 nm in width). This modulator couples the light from conventional Si-wire waveguides (400 nm×220 nm) through a unique highly efficient

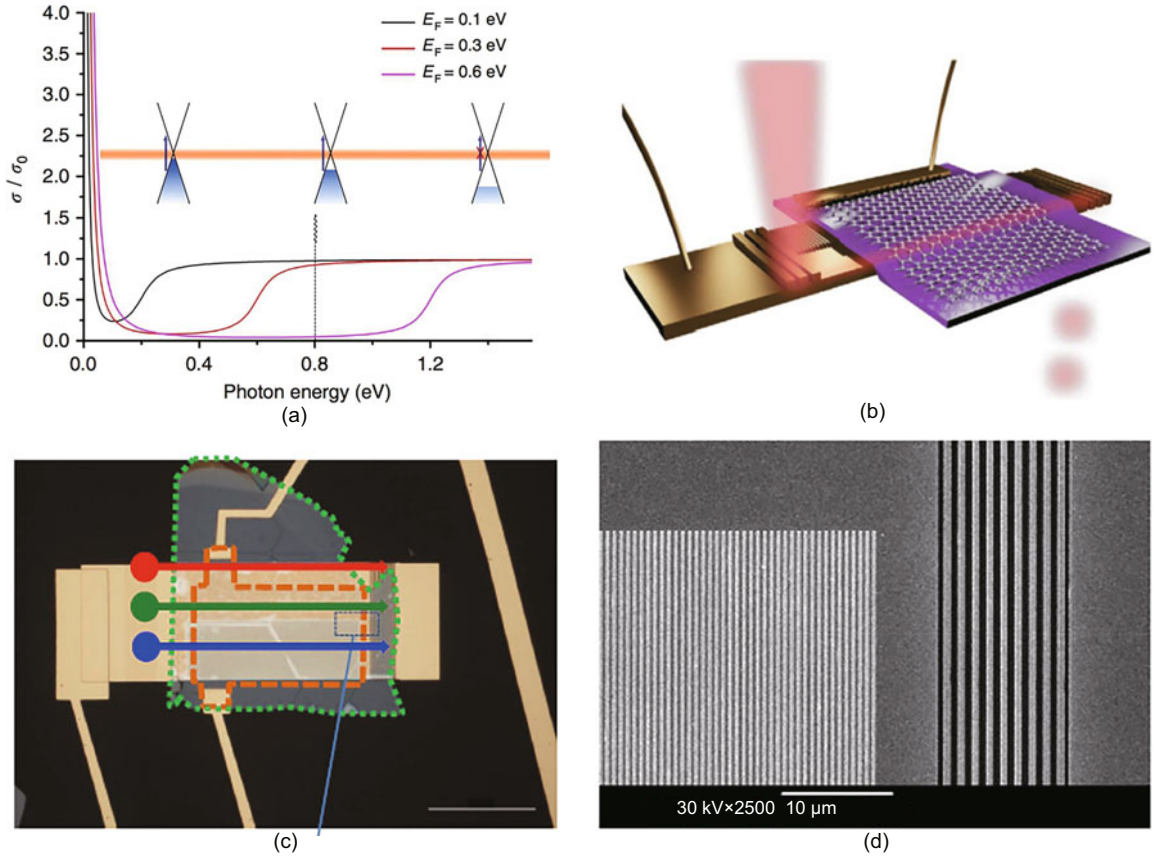


**Fig. 9 Optical Pauli blocking expressed in terms of graphene relative conductivity (a), 3D rendering of the wedge plasmon mode based hybrid graphene plasmonic waveguide (b), the optical micrograph of a typical hybrid graphene plasmonic modulator studied in this work (c), and a scanning electron micrograph of an area shown in (c) by the dotted box that shows a corrugated waveguide and the semitransparent decoupling grating (d) (Ansell et al. (2015), licensed under CC BY 4.0). In (c), red, green, and blue arrows represent wedge plasmons (WP), flat plasmons (FP), and corrugated plasmons (CP) modes, respectively; the area enclosed by the green dotted line represents hBN; the area enclosed by the dotted brown line represents graphene (scale bar: 50 mm). References to color refer to the online version of this figure**

mode converter. Such an ultrahigh-speed all-optic modulator has a response time of 2.2 ps at 1550 nm while the required pump pulse energy is 155 fJ, which is the smallest value yet reported for pico-second all-optical modulation. In addition, the device length including the mode converters is only 12 μm.

Graphene SPP devices possess many superior characteristics, such as deep-subwavelength field confinement in the mid-infrared (mid-IR) spectral range (2–20 μm), excellent tunability, and low ohmic loss (Xiao et al., 2017). Prototypes of a graphene plasmonic silicon modulator based on a slot waveguide (Ding et al., 2017; Hu and Wang, 2017) and directional coupler (Shin and Kim, 2015) have been proposed, through few experimental results.

## 6 Challenges and future perspectives

The modulator is an important component in silicon-based integrated circuits and on-chip optical interconnection systems. Owing to the excellent optical and electrical properties of the material, graphene opens up a promising way to realize various kinds of high-performance graphene-based silicon modulators, including E-O graphene-silicon modulators, T-O graphene-silicon modulators, all-optical graphene-silicon modulators, and graphene-plasmonic modulators. The typical studies in relation to these modulators over the last decade are summarized in Table 1. Compared to well-developed traditional silicon-based modulators, graphene modulators exhibit distinct advantages, i.e., enabling

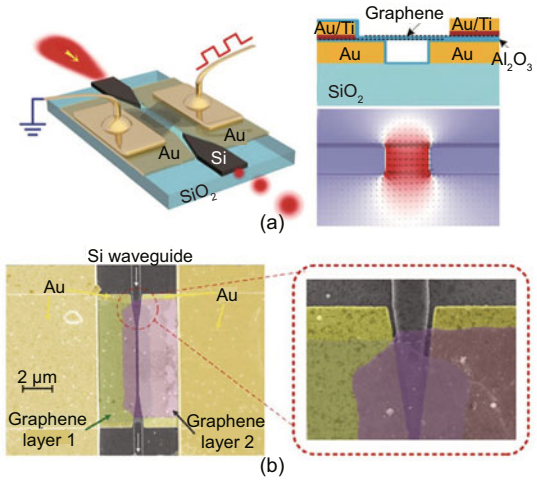


**Fig. 10 Structure of the designed graphene-plasmonic hybrid slot waveguide modulator: (a) 3D schematic of the device (left), cross-section of waveguide configurations (with air being the upper cladding) (right top), and the plasmonic slot mode profile indicating how the electromagnetic field is strongly confined to the slot region (right bottom); (b) false-color SEM image of the fabricated graphene-plasmonic slot hybrid waveguide in (a) (left), and a zoom-in on the coupling part of the fabricated device (right) (reprinted from Ding et al. (2017), Copyright 2017, with permission from Royal Society of Chemistry)**

high modulation speed, broad optical bandwidth, small footprint, low power consumption, and seamless integration with CMOS electronics. However, there still exist several challenges in fully exploiting the superb characteristics of graphene. Moreover, the device performance is still far away from the theoretical calculations and simulation predictions in several respects.

T-O and all-optical graphene-based silicon modulators are relatively simple for implementing optical modulation by graphene-silicon hybrid structures. However, both types of graphene modulators face a limited operation speed of only several Megahertz. Therefore, these two modulation schemes show only application potential in low-speed and high-efficiency optical modulators or in optical switching.

E-O modulation can realize direct conversion between high-speed electrical signals and optical signals. It is also the most attractive scheme for graphene-based silicon modulators. Many studies have investigated this type of graphene modulator experimentally or theoretically, exploiting and pursuing higher device performances. Up to now, the two most important performance metrics of modulators, which are the E-O bandwidths and modulation efficiency, can reach 35 GHz and 0.28 V·cm respectively for graphene modulators, and these are still much lower than the theoretical values. Capacitance is the main factor for the depressed modulation speed of the graphene E-O modulator.

Increasing the thickness of the oxide insulation layer can help improve the cut-off frequency of the capacitor. Thus, the device bandwidth can be promoted. However, as the oxide layer gets thicker, the required driven voltages may become higher and the modulation efficiency and power consumption would be degenerated. Since the graphene is transferred to the upper surface of the silicon waveguide, the interaction between graphene and the propagation optical mode is rather weak, which results in low modulation efficiency. While this factor can be improved by embedding the graphene layers into the waveguide core as well as adding graphene layers, it places greater demand on the fabrication procedure. In addition, the transfer process determines the quality of the graphene, reflected in the mobility and the completeness of the graphene layer. Therefore, this factor also has a significant impact on the performance of the modulator. To further improve the device performance, these factors as defined above should be taken into account and properly dealt with.

Graphene-plasmonic modulators combine the advantages of graphene and plasmonic, thus boosting the device performance in terms of modulation efficiency, power consumption, and compactness. Yet, it is quite difficult to manufacture this type of graphene modulator; therefore, few experimental demonstrations have been reported. The hybrid integration of the metal layer on silicon also introduces an additional optical propagation loss. Meanwhile, such a configuration makes compatibility with standard CMOS techniques difficult. To reduce the device loss, one practicable solution is to use resonant structures or slow wave structures to reduce the footprint. Such a resonant structure has already been demonstrated for the plasmonic silicon modulator.

So far, graphene-based silicon modulators have made great progress at an extremely fast pace, ranging across material modulation principles, conceptual devices, fabrication processes, and primary experimental demonstrations. Nevertheless, there is still a significant demand for performance

**Table 1 Reported works of electro-optical (E-O), thermo-optical (T-O), all-optical, and plasmonic graphene silicon modulators**

| Modulator | Scheme | Size | Modulation efficiency | Year | Reference |
|---|---|---|---|---|---|
| SLG Si strip waveguide (E) | E-O (EA) | 25 μm$^2$ | 0.1 dB/μm | 2011 | Liu et al. (2011) |
| DLG Si strip waveguide (E) | E-O (EA) | 40 μm (length) | 0.16 dB/μm | 2012 | Liu et al. (2012) |
| DLG $Si_3N_4$ microring (E) | E-O (EA) | 40 μm (radius) | 15 dB@10 V | 2015 | Phare et al. (2015) |
| DLG Si slot Mach-Zehnder (T) | E-O (ER) | 100 μm (length) | 0.063 V·cm | 2016 | Phatak et al. (2016) |
| SLG Si rib Mach-Zehnder (E) | E-O (ER) | 300 μm (length) | 0.28 V·cm | 2017 | Sorianello et al. (2018) |
| SLG Si rib Mach-Zehnder (E) | E-O (ER) | 40 μm (length) | 0.13 V·cm | 2018 | Shu et al. (2018b) |
| SLG Si Mach-Zehnder (E) | T-O | 120 μm (length) | 0.064 nm/mW | 2014 | Yu et al. (2014) |
| SLG Si microring (E) | T-O | 10 μm$^2$ | 0.1 nm/mW | 2015 | Gan et al. (2015) |
| SLG $Si_3N_4$ microring (E) | T-O | 60 μm (radius) | 0.008 nm/mW | 2017 | Qiu et al. (2017) |
| SLG Si crystal cavity (E) | All-optical | — | 0.06 nm/mW | 2015 | Shi et al. (2015) |
| SLG $Si_3N_4$ microring (E) | All-optical | — | 0.023 nm/mW | 2017 | Gao et al. (2017) |
| SLG-hBN-Si waveguide (T) | Plasmonic | 9 μm (length); 1.3 μm$^2$ | 21.7 dB@1.8 V | 2015 | Shin and Kim (2015) |
| SLG-hBN-SLG waveguide (T) | Plasmonic | 3 μm (length) | 39.75 dB@3.13 V | 2016 | Chen et al. (2016) |
| DLG slot waveguide (E) | Plasmonic | — | 2.1 dB@7.5 V | 2017 | Ding et al. (2017) |
| DLG plasmonic slot waveguide (T) | Plasmonic | 363 nm (length) | 3 dB | 2017 | Hu and Wang (2017) |
| SLG plasmonic waveguide (E) | Plasmonic | 60 nm×40 nm | 2.5 dB | 2018 | Ono et al. (2018) |

T: theoretical or simulation results; E: experimental results. SLG: single-layer graphene; DLG: double-layer graphene; hBN: hexagonal boron nitride; EA: electric-absorption modulation; ER: electric-refraction modulation

improvement and application practicality, which means a continuous effort to exploit effective mechanisms, practical techniques, and novel modulation configurations. Given this, graphene-based silicon modulators still encompass a broad development space and many opportunities to compete with existing mature technologies in the future.

## References


Andersen DR, 2010. Graphene-based long-wave infrared TM surface plasmon modulator. *J Opt Soc Am B*, 27(4):818-823. https://doi.org/10.1364/josab.27.000818

Ansell D, Radko IP, Han Z, et al., 2015. Hybrid graphene plasmonic waveguide modulators. *Nat Commun*, 6:8846. https://doi.org/10.1038/ncomms9846

Balandin AA, Ghosh S, Bao WZ, et al., 2008. Superior thermal conductivity of single-layer graphene. *Nano Lett*, 8(3):902-907. https://doi.org/10.1021/nl0731872

Chen L, Doerr CR, Dong P, et al., 2011. Monolithic silicon chip with 10 modulator channels at 25 Gbps and 100-GHz spacing. *Opt Expr*, 19(26):B946-B951. https://doi.org/10.1364/oe.19.00b946

Chen L, Dong P, Chen YK, 2012. Chirp and dispersion tolerance of a single-drive push-pull silicon modulator at 28 Gb/s. *IEEE Photon Technol Lett*, 24(11):936-938. https://doi.org/10.1109/lpt.2012.2191149

Chen X, Wang Y, Xiang YJ, et al., 2016. A broadband optical modulator based on a graphene hybrid plasmonic waveguide. *J Lightw Technol*, 34(21):4948-4953. https://doi.org/10.1109/jlt.2016.2612400

Cocorullo G, Rendina I, 1992. Thermo-optical modulation at 1.5μm in silicon etalon. *Electron Lett*, 28(1):83-85. https://doi.org/10.1049/el:19920051

Dalir H, Xia Y, Wang Y, et al., 2016. Athermal broadband graphene optical modulator with 35 GHz speed. *ACS Photon*, 3(9):1564-1568. https://doi.org/10.1021/acsphotonics.6b00398

Das S, Salandrino A, Wu JZ, et al., 2015. Near-infrared electro-optic modulator based on plasmonic graphene. *Opt Lett*, 40(7):1516-1519. https://doi.org/10.1364/ol.40.001516

Ding Y, Zhu X, Xiao SS, et al., 2015. Effective electro- optical modulation with high extinction ratio by a graphene-silicon microring resonator. *Nano Lett*, 15(7):4393-4400. https://doi.org/10.1021/acs.nanolett.5b00630

Ding Y, Guan X, Zhu X, et al., 2017. Efficient electro-optic modulation in low-loss graphene-plasmonic slot waveguides. *Nanoscale*, 9(40):15576-15581. https://doi.org/10.1039/c7nr05994a

Dionne JA, Diest K, Sweatlock LA, et al., 2009. PlasMOStor: a metal-oxide-Si field effect plasmonic modulator. *Nano Lett*, 9(2):897-902. https://doi.org/10.1021/nl803868k

Gan S, Cheng CT, Zhan YH, et al., 2015. A highly efficient thermo-optic microring modulator assisted by graphene. *Nanoscale*, 7(47):20249-20255. https://doi.org/10.1039/c5nr05084g

Gao Y, Zhou W, Sun XK, et al., 2017. Cavity-enhanced thermo-optic bistability and hysteresis in a graphene-on-$Si_3N_4$ ring resonator. *Opt Lett*, 42(10):1950-1953. https://doi.org/10.1364/ol.42.001950

Gosciniak J, Tan DTH, 2013a. Graphene-based waveguide integrated dielectric-loaded plasmonic electro-absorption modulators. *Nanotechnology*, 24(18):185202. https://doi.org/10.1088/0957-4484/24/18/185202

Gosciniak J, Tan DTH, 2013b. Theoretical investigation of graphene-based photonic modulators. *Sci Rep*, 3:1897. https://doi.org/10.1038/srep01897

Haffner C, Heni W, Fedoryshyn Y, et al., 2015. All-plasmonic Mach-Zehnder modulator enabling optical high-speed communication at the microscale. *Nat Photon*, 9(8):525-528. https://doi.org/10.1038/nphoton.2015.127

Hanson GW, 2008. Dyadic Green's functions and guided surface waves for a surface conductivity model of graphene. *J Appl Phys*, 103(6):064302. https://doi.org/10.1063/1.2891452

Hu X, Wang J, 2017. High figure of merit graphene modulator based on long-range hybrid plasmonic slot waveguide. *IEEE J Quant Electron*, 53(3):7200308. https://doi.org/10.1109/jqe.2017.2686371

Jones R, Liao L, Liu AS, et al., 2004. Optical characterization of 1-GHz silicon-based optical modulator. *Proc SPIE*, 5451:8-15. https://doi.org/10.1117/12.565628

Kim JT, Chung KH, Choi CG, 2013. Thermo-optic mode extinction modulator based on graphene plasmonic waveguide. *Opt Expr*, 21(13):15280-15286. https://doi.org/10.1364/oe.21.015280

Koeber S, Palmer R, Lauermann M, et al., 2015. Femtojoule electro-optic modulation using a silicon-organic hybrid device. *Light Sci Appl*, 4(2):e255. https://doi.org/10.1038/lsa.2015.28

Lao J, Tao J, Wang QJ, et al., 2014. Tunable graphene-based plasmonic waveguides: nano modulators and nano attenuators. *Laser Photon Rev*, 8(4):569-574. https://doi.org/10.1002/lpor.201300199

Li TT, Zhang JL, Yi HX, et al., 2013. Low-voltage, high speed, compact silicon modulator for BPSK modulation. *Opt Expr*, 21(20):23410-23415. https://doi.org/10.1364/oe.21.023410

Li W, Chen BG, Meng C, et al., 2014. Ultrafast all-optical graphene modulator. *Nano Lett*, 14(2):955-959. https://doi.org/10.1021/nl404356t

Li ZQ, Henriksen EA, Jiang Z, et al., 2008. Dirac charge dynamics in graphene by infrared spectroscopy. *Nat Phys*, 4(7):532-535. https://doi.org/10.1038/nphys989

Li ZY, Yu NF, 2013. Modulation of mid-infrared light using graphene-metal plasmonic antennas. *Appl Phys Lett*, 102(13):131108. https://doi.org/10.1063/1.4800931

Liu AS, Jones R, Liao L, et al., 2004. A high-speed silicon optical modulator based on a metal-oxide-semiconductor capacitor. *Nature*, 427(6975):615-618. https://doi.org/10.1038/nature02310

Liu M, Yin XB, Ulin-Avila E, et al., 2011. A graphene-based broadband optical modulator. *Nature*, 474(7349):64-67. https://doi.org/10.1038/nature10067

Liu M, Yin XB, Zhang X, 2012. Double-layer graphene optical modulator. *Nano Lett*, 12(3):1482-1485. https://doi.org/10.1021/nl204202k

Liu WJ, Asheghi M, 2005. Thermal conduction in ultrathin pure and doped single-crystal silicon layers at high temperatures. *J Appl Phys*, 98(12):123523. https://doi.org/10.1063/1.2149497

Miller DAB, 2009. Device requirements for optical interconnects to silicon chips. *Proc IEEE*, 97(7):1166-1185. https://doi.org/10.1109/jproc.2009.2014298

Miller DAB, 2012. Energy consumption in optical modulators for interconnects. *Opt Expr*, 20(S2):A293-A308. https://doi.org/10.1364/oe.20.00a293

Mohsin M, Schall D, Otto M, et al., 2014. Graphene based low insertion loss electro-absorption modulator on SOI waveguide. *Opt Expr*, 22(12):15292-15297. https://doi.org/10.1364/oe.22.015292

Mohsin M, Neumaier D, Schall D, et al., 2015. Experimental verification of electro-refractive phase modulation in graphene. *Sci Rep*, 5:10967. https://doi.org/10.1038/srep10967

Novoselov KS, Geim AK, Morozov SV, et al., 2004. Electric field effect in atomically thin carbon films. *Science*, 306(5696):666-669. https://doi.org/10.1126/science.1102896

Ono M, Hata M, Tsunekawa M, et al., 2018. Ultrafast and energy-efficient all-optical modulator based on deep-subwavelength graphene-loaded plasmonic waveguides. Conf on Lasers and Electro-Optics, Article FF2L.4. https://doi.org/10.1364/cleo_qels.2018.ff2l.4

Phare CT, Lee YHD, Cardenas J, et al., 2015. Graphene electro-optic modulator with 30 GHz bandwidth. *Nat Photon*, 9(8):511-514. https://doi.org/10.1038/nphoton.2015.122

Phatak A, Cheng ZZ, Qin CY, et al., 2016. Design of electro-optic modulators based on graphene-on-silicon slot waveguides. *Opt Lett*, 41(11):2501-2504. https://doi.org/10.1364/ol.41.002501

Pop E, Varshney V, Roy AK, 2012. Thermal properties of graphene: fundamentals and applications. *MRS Bull*, 37(12):1273-1281. https://doi.org/10.1557/mrs.2012.203

Qiu CY, Gao WL, Vajtai R, et al., 2014. Efficient modulation of 1.55 μm radiation with gated graphene on a silicon microring resonator. *Nano Lett*, 14(12):6811-6815. https://doi.org/10.1021/nl502363u

Qiu CY, Yang YX, Li C, et al., 2017. All-optical control of light on a graphene-on-silicon nitride chip using thermo-optic effect. *Sci Rep*, 7(1):17046. https://doi.org/10.1038/s41598-017-16989-9

Reed GT, Mashanovich G, Gardes FY, et al., 2010. Silicon optical modulators. *Nat Photon*, 4(8):518-526. https://doi.org/10.1038/nphoton.2010.179

Shi Z, Gan L, Xiao TH, et al., 2015. All-optical modulation of a graphene-cladded silicon photonic crystal cavity. *ACS Photon*, 2(11):1513-1518. https://doi.org/10.1021/acsphotonics.5b00469

Shin JS, Kim JT, 2015. Broadband silicon optical modulator using a graphene-integrated hybrid plasmonic waveguide. *Nanotechnology*, 26(36):365201. https://doi.org/10.1088/0957-4484/26/36/365201

Shu HW, Tao YS, Jin M, et al., 2018a. A real-time tunable arbitrary power ratios graphene based power divider. *Sci China Inform Sci*, 61(8):080408. https://doi.org/10.1007/s11432-018-9431-0

Shu HW, Su ZT, Huang L, et al., 2018b. Significantly high modulation efficiency of compact graphene modulator based on silicon waveguide. *Sci Rep*, 8(1):991. https://doi.org/10.1038/s41598-018-19171-x

Soref R, Larenzo J, 1986. All-silicon active and passive guided-wave components for $\lambda$=1.3 and 1.6 μm. *IEEE J Quant Electron*, 22(6):873-879. https://doi.org/10.1109/jqe.1986.1073057

Sorianello V, Midrio M, Romagnoli M, 2015. Design optimization of single and double layer graphene phase modulators in SOI. *Opt Expr*, 23(5):6478-6490. https://doi.org/10.1364/oe.23.006478

Sorianello V, de Angelis G, Cassese T, et al., 2016. Complex effective index in graphene-silicon waveguides. *Opt Expr*, 24(26):29984-29993. https://doi.org/10.1364/oe.24.029984

Sorianello V, Midrio M, Contestabile G, et al., 2018. Graphene-silicon phase modulators with gigahertz bandwidth. *Nat Photon*, 12(1):40-44. https://doi.org/10.1038/s41566-017-0071-6

Thomson D, Zilkie A, Bowers JE, et al., 2016. Roadmap on silicon photonics. *J Opt*, 18(7):073003. https://doi.org/10.1088/2040-8978/18/7/073003

Wang F, Zhang YB, Tian CS, et al., 2008. Gate-variable optical transitions in graphene. *Science*, 320(5873):206-209. https://doi.org/10.1126/science.1152793

Xiao TH, Cheng ZZ, Goda K, 2017. Graphene-on-silicon hybrid plasmonic-photonic integrated circuits. *Nanotechnology*, 28(24):245201. https://doi.org/10.1088/1361-6528/aa7128

Xu C, Jin YC, Yang LZ, et al., 2012. Characteristics of electro-refractive modulating based on graphene-oxide-silicon waveguide. *Opt Expr*, 20(20):22398-22405. https://doi.org/10.1364/oe.20.022398

Xu F, Das S, Gong Y, et al., 2015. Complex refractive index tunability of graphene at 1550 nm wavelength. *Appl Phys Lett*, 106(3):031109. https://doi.org/10.1063/1.4906349

Xu ZZ, Qiu CY, Yang YX, et al., 2017. Ultra-compact tunable silicon nanobeam cavity with an energy-efficient graphene micro-heater. *Opt Expr*, 25(16):19479-19486. https://doi.org/10.1364/oe.25.019479

Yamane T, Nagai N, Katayama SI, et al., 2002. Measurement of thermal conductivity of silicon dioxide thin films using a 3$\omega$ method. *J Appl Phys*, 91(12):9772. https://doi.org/10.1063/1.1481958

Yan HG, Li XS, Chandra B, et al., 2012. Tunable infrared plasmonic devices using graphene/insulator stacks. *Nat Nanotechnol*, 7(5):330-334. https://doi.org/10.1038/nnano.2012.59

Yan SQ, Zhu XL, Frandsen LH, et al., 2017. Slow-light-enhanced energy efficiency for graphene microheaters on silicon photonic crystal waveguides. *Nat Commun*, 8:14411. https://doi.org/10.1038/ncomms14411

Ye SW, Yuan F, Zou XH, et al., 2017. High-speed optical phase modulator based on graphene-silicon waveguide. *IEEE J Sel Top Quant Electron*, 23(1):3400105. https://doi.org/10.1109/jstqe.2016.2545238

Yin YL, Li J, Xu Y, et al., 2018. Silicon-graphene photonic devices. *J Semicond*, 39(6):061009. https://doi.org/10.1088/1674-4926/39/6/061009

Yu LH, Dai DX, He SL, 2014. Graphene-based transparent flexible heat conductor for thermally tuning nanophotonic integrated devices. *Appl Phys Lett*, 105(25):251104. https://doi.org/10.1063/1.4905002

Yu LH, Yin YL, Shi YC, et al., 2016. Thermally tunable silicon photonic microdisk resonator with transparent graphene nanoheaters. *Optica*, 3(2):159-166. https://doi.org/10.1364/optica.3.000159